MODELLING AND EXPERIMENTAL VERIFICATION OF DELAMINATION CRACK GROWTH IN AN AIR-PLASMA-SPRAYED THERMAL BARRIER COATING

H. Brodin[1], M. Jinnestrand[1], S. Sjöström[1,2]
[1]Dept. of Mechanical Engineering, Linköping University, SE-581 83 LINKÖPING, Sweden
[2]Dept. GRCR, SIEMENS, SE-612 83 FINSPÅNG, Sweden

Abstract

A model for thermal barrier coating (TBC) fatigue life is presented. The model is based on the growth of delamination cracks in or near the top coat/bond coat interface, governed by a Paris-like law. In parallel with the calculations a test series has been run in order to show the actual coating fatigue behaviour. Test results are compared with those from the modelling work. The tests reveal that interface cracks initiate already after 100 cycles and continue to grow. Upon further cycling the interface cracks tend to kink out into the ceramic top coat. It was observed that the crack growth retards during later stages of the process, independent on whether an interface crack or an interface-near kink crack is considered.

Keywords: TBC, delamination, crack growth, thermal fatigue, life modelling

Introduction

Thermal barrier coatings (TBCs) are commonly used in hot parts (combustor liners and turbine vanes and blades) of land-based gas turbines and aeroengines. From a fatigue point of view, these two applications are rather different: Land-based gas turbines typically run at constant and maximum load for several hours, whereas aeroengines (particularly military engines) typically run for short time periods but with rapid changes in power output.

A thermal barrier coating consists of a metallic bond coat (BC) and a ceramic top coat (TC). The TC serves as a thermal insulation, whereas the BC provides improved adhesion for the ceramic TC and protects the substrate metal from oxidation by itself forming an adherent thermally grown oxide (TGO) scale at the BC/TC interface.

A physically sound TBC life model must incorporate influence on fatigue life from phenomena observed in ex-serviced gas turbine components. Of large importance are factors such as oxidation behaviour [1, 2, 3, 4], TBC interface geometry [3, 4] and residual stress state [4, 5]. The main reason for TBC failure is delamination. The common opinion is that cracks initiate and grow at or near the TGO at the TC/BC interface. Several studies have proved this. However, at least three fracture types exist, namely white fracture with cracks initiating and propagating in the TC [4, 6], black fracture with initiation and propagation at the TC/BC interface (*i.e.*, at the interface of or within the TGO [7, 8]). and a mixture of the white and black types, [9, 10].

Material

In the present work an air plasma sprayed (APS) TBC has been studied. The aim has been to extract interface delamination data from thermal cyclic fatigue (TCF) tests. Fatigue tests have

been done on a TBC system with an yttria-stabilised zirconia (ZrO_2 7wt% Y_2O_3) TC in combination with a nickel-based (Ni-23Co-17Cr-12.5Al-0.5Y) BC. The TC thickness was 350µm and the BC thickness 150 µm. The substrate material was the nickel-base superalloy H230 from Haynes International. 50x30x5mm test coupons were machined from H230 sheet material and grit-blasted. After this the coating was applied. The initial microstructure is shown in Fig. 1.

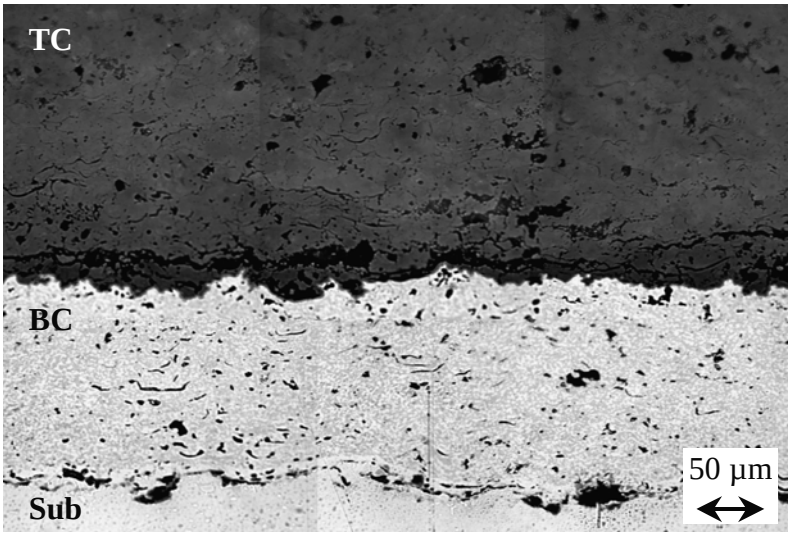

FIGURE 1. The thermal barrier coating system used in the present study. Dark grey top coat (upper), bright bond coat with internal oxide streaks (middle) and substrate (lower). Black areas in the top coat are porosities.

Experimental procedure

The TCF tests were carried out in a thermal cycle furnace, ECF 13-12F, equipped with a program cycle fatigue controller PLC MAC10. During fatigue testing the furnace temperature was kept at a constant temperature of 1100°C, while the specimen holder was automatically moved between the furnace and the cooling equipment. Cooling to 100°C was achieved with compressed air. All test coupons were cooled at an average cooling rate of 84°C/min. During cooling the airflow was adjusted so that the temperature deviation between individual samples was kept below 40°C corresponding to $\Delta T < 6\%$. In order to detect presence, location and growth of delamination cracks during the thermal cycling, specimens were removed from the TCF equipment after 100, 300, 400, 500, 600, 700 and 886 cycles, respectively, and inspected by light optical microscopy / image analysis after sectioning and sample preparation.

The development of delamination damage during thermal cyclic fatigue is influenced by which of the three above-mentioned delamination and spallation mechanism is active. This, in turn, depends on several factors, such as coating quality (coating application technique), development of TGOs at the TC/BC interface (formation of alumina or more voluminous oxides) and TC/BC interface geometry (stress state and interface adhesion). It is convenient to establish an expression that describes percentage of interface damage according to a new interface damage parameter *D*:

$$D = \frac{\sum_p l_{c,i} + \sum_q l_{c,k} + \sum_r l_{c,t}}{L} \tag{1}$$

where D is the observed percentage of interface damage due to delamination, $l_{c,i}$ is the length of individual interface cracks p, $l_{c,k}$ is the length of individual kink cracks q and $l_{c,t}$ is the length of individual top coat cracks r, and L is the observed section length..

Fracture-mechanical analysis

The cracks observed in the TBC are analysed by a fracture mechanical approach. General references on interface cracks are Hutchinson and Suo [11] and Rice [12].

In our case, the energy release rate G is first calculated by a virtual crack extension method. From the relative crack flank displacement,

$$\delta_2 + i\delta_1 = \frac{8(K_1 + iK_2)}{(1+2i\varepsilon)\cosh(\pi\varepsilon)}\sqrt{\frac{r}{2\pi}}\,\frac{r^{i\varepsilon}}{\hat{E}}, \tag{2}$$

the ratio K_1 / K_2 of the stress intensity factors K_1 and K_2 is computed. Knowing this, K_1 and K_2 can finally be computed from the equation

$$G = \frac{1}{H}(K_1^2 + K_2^2). \tag{3}$$

In the above equations,

$$\varepsilon = \frac{1}{2\pi}\log\left(\left(\frac{\mu_{TC}}{G_{TC}} + \frac{1}{G_{BC}}\right)/\left(\frac{\mu_{BC}}{G_{BC}} + \frac{1}{G_{TC}}\right)\right), \tag{4}$$

$$\frac{1}{\hat{E}} = \frac{1}{2}\left(\frac{1-\nu_{TC}^{\,2}}{E_{TC}} + \frac{1-\nu_{BC}^{\,2}}{E_{BC}}\right), \tag{5}$$

and

$$H = \hat{E}\cdot\cosh^2(\pi\varepsilon). \tag{6}$$

Fracture-mechanical analyses were made for an interface crack in the TGO layer and for a delamination crack in the top coat just above the TGO layer, growing parallel to the layer.

Plane strain was assumed in the finite element simulation. The TC/BC interface was modelled as a sinusoidal curve with period half-length L = 70 μm and double amplitude H = 20 μm. The TBC system was assumed to be stress-free at high temperature and loaded by a thermal cycle between 1100°C and 100°C.

Repeated FE simulations have been performed for different crack lengths and three levels of TGO thickness (namely, 4, 6 and 8 μm). The results from these simulations have been stored in a database for use during the integration of the life model to be described later. A few examples of the results are shown in Fig. 6.

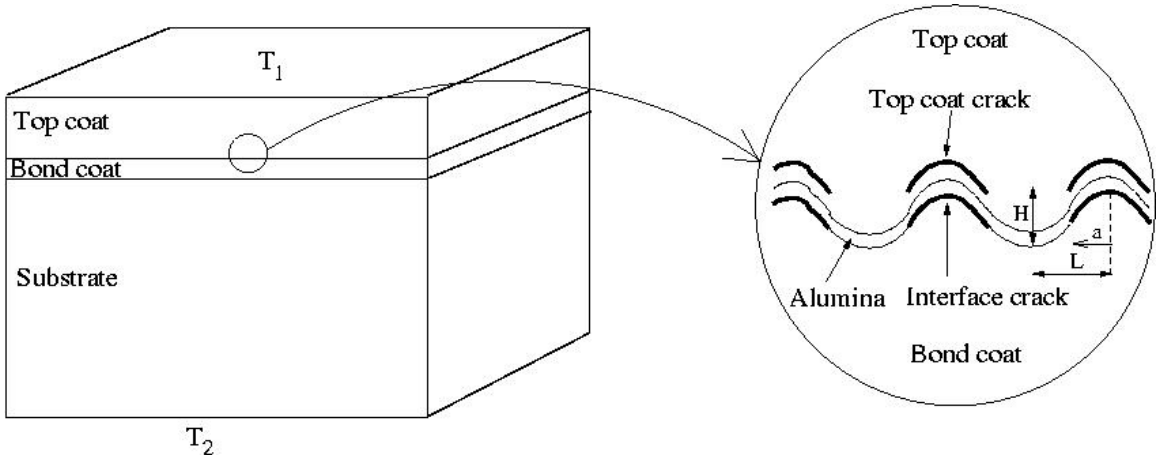

FIGURE 2: Model of the TBC system. The delamination crack paths used in the FE simulations are shown in the right part of the figure.

Life model formulation

Only very few articles have been published that take a fracture-mechanical model of a TBC all the way to a finished life model. The articles by Ahrens *et al*. [13] and Traeger *et al*. [14] can, however, be mentioned.

The life model developed in this article is based on a Paris' law. A modification is, however, needed since the delamination crack in the TGO/TC interface does not necessarily follow a path which makes $K_{II} = 0$. Instead, the crack is basically confined to following a path parallel to the TGO layer, which leads to a mixed mode I/mode II case. When *a/L* is of the order of 0.5 or larger and mode II dominates, we get shearing of the crack, probably contact between the (rather rough) crack flanks and lower crack growth rate (*cf* Fig. 6).

The Paris' law formulation developed is based on the energy release rate, *i.e.*,

$$\frac{dD}{dN} = C_2(\lambda G)^{n_2}, \tag{7}$$

where λ is a function that takes into account the energy dissipation during shearing deformation of the crack. Obviously, $0 < \lambda < 1$. A proposed formulation is

$$\lambda = 1 - (1 - \lambda_0)\left(\frac{2}{\pi}\tan^{-1}\left(\frac{K_2}{K_1}\right)\right)^m \tag{8}$$

where λ_0 and *m* are material parameters to be determined.

Integration of the life model

The integration of (7) can formally be written as

$$N = N_0 + \int_{D_0}^{D_{cr}} \frac{\mathrm{d}\,D}{f(\Delta G, \Delta K_1, \Delta K_2, \ldots)} \tag{9}$$

where N_0 is the number of cycles to crack initiation, D_0 is the (assumed) damage at the instant of start of crack growth and D_{cr} is the (assumed) damage at final failure. In the integration of the life model, D_0 has been chosen = 0.1 and $D_{cr} = 0.9$. The 'norm' radius r, needed in Eq. (2) has been taken as r = 1.2 μm.

The stress intensity factors depend, among other things, on the TGO thickness. It is therefore necessary to compute the TGO thickness as a function of time and temperature. As long as only alumina forms in the TGO, the thickness h_{TGO} of the TGO layer can be calculated as

$$h_{TGO} = Ce^{\frac{-Q}{RT}}\sqrt{t}\,, \tag{10}$$

where Q is the activation energy, R is the gas constant, T is the Kelvin temperature, t is the time and C is a constant. In our case, Q = 79000 J/m, R = 8.3141 J/mole·K. and C = $6.1345 \cdot 10^6$. m/s$^{1/2}$.

Life model parameter estimation

The parameters in the life models have been estimated by an optimization procedure, using a weighted least squares method.

Results

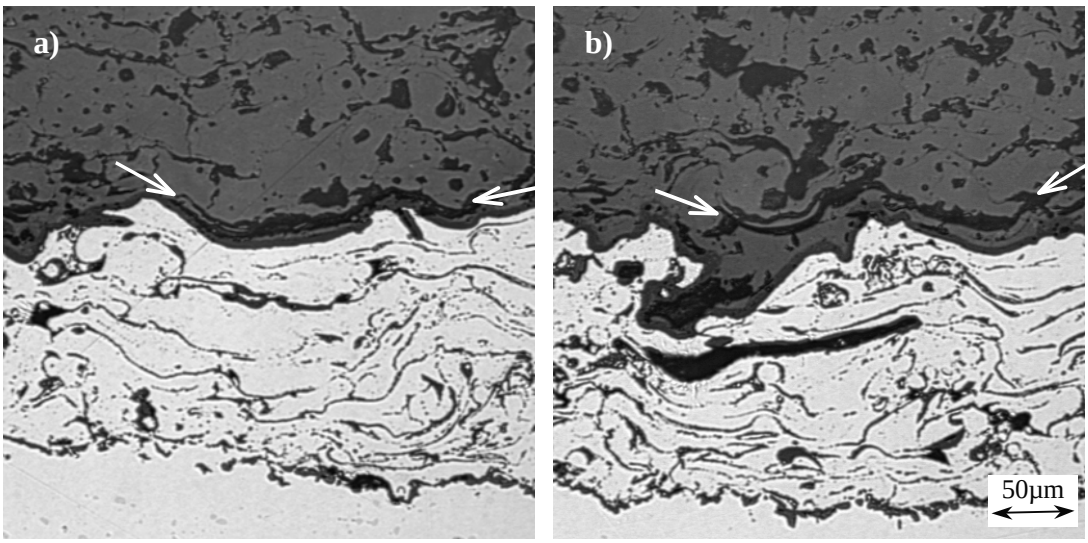

FIGURE 3. Typical micrographs of delamination cracks found after thermal TCF testing (as indicated by arrows). Figure a) shows an interface crack, in figure b) an interface near crack is depicted.

Fractographic investigation

In the present study the TCF tests were interrupted after 886 cycles. At this point of time no visible damage was detectable, *i.e*. no spallation had taken place. By investigation of TBC cross sections it was, however, possible to observe two parallel TBC delamination mechanisms, namely, interface cracks and mixed cracks. The latter crack type is initiated at the

TC/BC interface. With time the cracks will kink out from the interface into the TC. Typical appearances of the two crack types found in the present study are presented in Fig. 3.

TCF testing

Results from measurements of average crack length c as a function of elapsed cycles N are presented in Fig. 4. Results are shown for interface cracks and kink cracks. These results are average values of measurements over a total interface length equal to 4.8 mm.

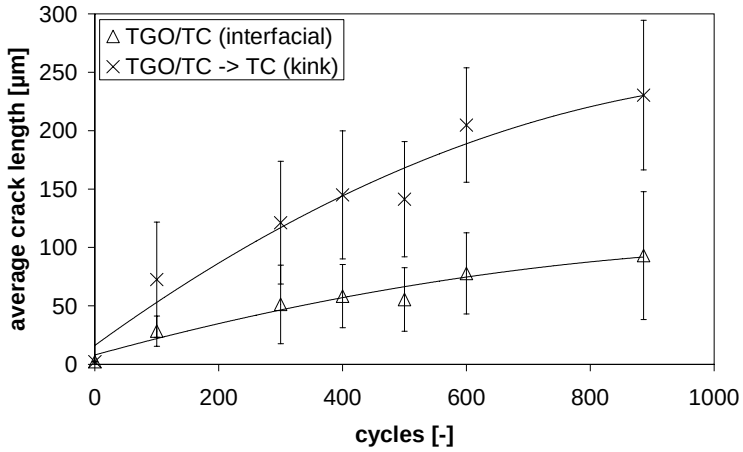

FIGURE 4. Measurements of average delamination crack length after TCF testing.

Results from calculations of interface damage D according to Eq. (1) are presented in Fig. 5. Triangles represent cracks that are initiated at the TC/BC interface and propagate at the interface. Crosses represent interface-near cracks (kink cracks) that have initiated at the interface. Circles represent the sum of the two contributions.

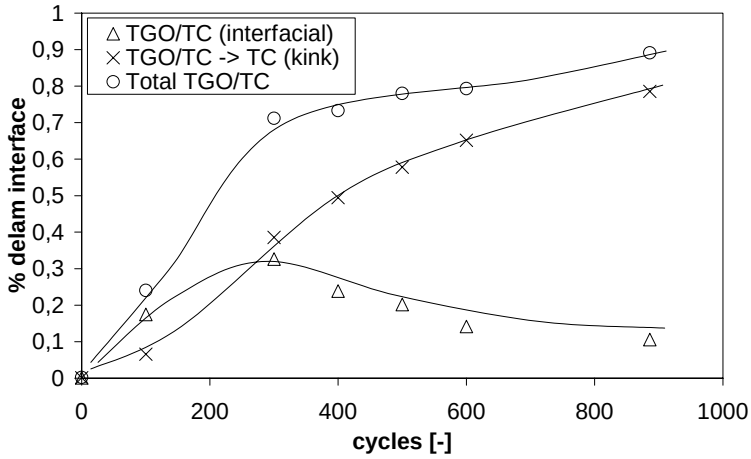

FIGURE 5. Development of interface damage. Delamination cracks of pure interface type (leading to white failure) and of kink type (mixed black/white cracks) are considered here.

Modelling, fracture mechanics

FE results showing K_1 and K_2 computed by Eqs. (2) through (7) are presented in Fig. 6. It can be seen that mode I dominates for small D, while mode II dominates for larger D. It is,

therefore, necessary to use a growth model for mixed-mode crack growth, as described above by Eqs. (7) and (8). The use of the computed K_1 and K_2 together with the life model described earlier using parameters from the optimisation process gives the results presented in Fig. 7.

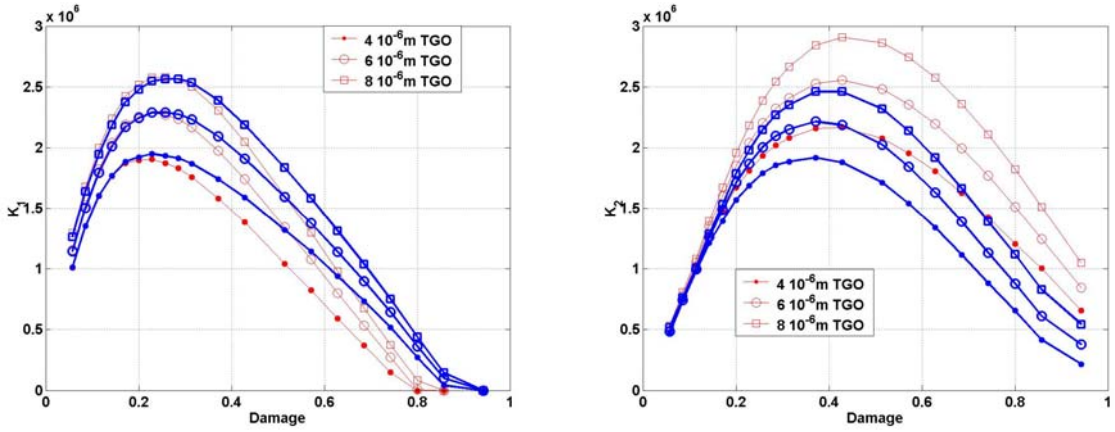

FIGURE 6. Fracture mechanical data of an interface crack. Left graph represents mode I FE results, right graph mode II results.

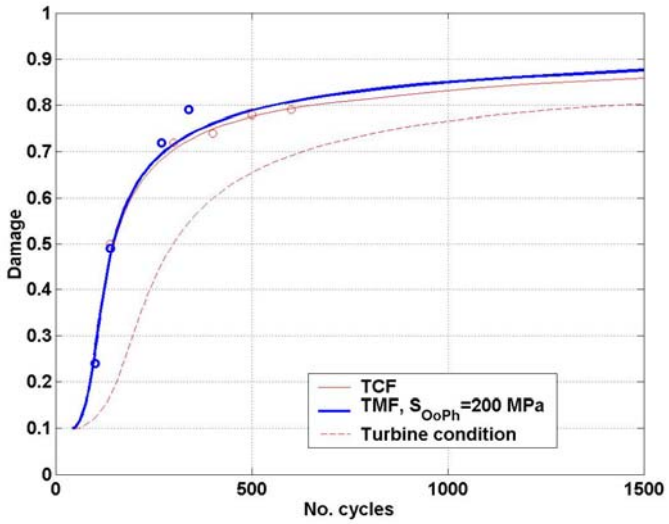

FIGURE 7. Results from parameter optimisation. Thin solid line: TCF test. Thick solid line: Out-of-phase thermomechanical fatigue (TMF) test with the same thermal cycle. Dashed line: Case with actual gas-turbine cycle data.

Summary and conclusions

The presented work aims at a physically founded fatigue life model for delamination crack growth in thermal barrier coatings in land-based gas turbines. In the present paper results from thermal fatigue testing and modelling work are presented. Two types of delamination cracks contribute to TBC spallation, namely interface cracks, initiated and propagated within the TC/BC interface oxide, and kink cracks, initiated at the interface but with propagation mainly within the ceramic top coat. Results show that the delamination process can be described as a cumulative damage due to adherence loss at the TC/BC interface. Testing re-

veals that the damage development is retarded and that substantial damage can be tolerated at the interface without TBC spallation. Modelling work indicates the same behaviour with an initial rapid crack growth and a long incubation period before final cracks coalesce and spallation occurs.

Conclusions:

- Interface adherence loss is caused by two crack types: interface cracks and interface-near cracks.
- It is possible to describe interface adherence loss as a damage parameter *D* that correlates total interface area to area detached due to delamination crack growth.
- A TBC life model can be based on Paris law with a K_I / K_{II} relation calculated from the energy release rate *G*.
- Modelling work shows that for short cracks, crack growth in mode I dominate. With increased crack length mode II crack growth will be controlling crack growth.

References

1. Schmitt-Thomas Kh G, Dietl U, *Surf. Coat. Technol.*, vol. **68/69**, 113-115, 1994.
2. Schmitt-Thomas Kh G, Hertter M, *Surf. Coat. Technol.*, vol. **120/121**, 84-88, 1999.
3. Anton R et.al., *European Federation of Corrosion publications*, no **27**, 340-356, 1999.
4. Vaßen R, Kerkhoff G, Stöver D, *Mater. Sci. Eng.*, vol. **A303**, 100-109, 2001.
5. Mumm D R, Evans G A, *Key Eng. Mater.*, vol. **197**, 199-230, 2001.
6. He M Y, Hutchinson J W, Evans G A, *Mater. Sci. Eng.*, vol. **A345**, 172-178, 2003.
7. Chen X, Hutchinson J W, He M Y, Evans G A, *Acta Mater.*, vol. **51**, 2017-2030, 2003.
8. Newaz G M, Nusier S Q, Chaudhury Z A, *J. Eng. Mater. Technol.*, vol. **120**, 149-153, 1998.
9. Schichting K W, Padture N P, Jordan E H, Gell M, *Mater. Sci. Eng.*, vol. **A342**, 120-130, 2003.
10. Quadakkers W J et.al., *In Elevated Temperature Coatings: Science and Technology III*, 119-130, San Diego, CF, February 28-March 4, 1999.
11. Hutchinson J W, Suo Z, *Advances in Applied Mechanics*, vol. **29**, 63-190, 1992.
12. Rice J R, *J. Appl. Mech*., vol. **55**, 98-103, 1988.
13. Ahrens M, Vaßen R, Stöver D, *Surface and Coatings Technology*, vol. **161**, 26-35, 2002.
14. Traeger F, Ahrens M, Vaßen R, Stöver D, *Materials. Science and Engineering*, vol. **A358**, 255-265, 2003.